

1 **Journal name:** Ecological Applications

2 **Manuscript type:** Article

3 **Manuscript title:** Multi-Factor Coral Disease Risk Forecasting for Early Warning and

4 Management

5 **Author Names:** *Jamie M Caldwell^{1,2}, Gang Liu³, Erick Geiger^{3,4}, Scott F Heron⁵, C Mark
6 Eakin⁶, Jacqueline De La Cour^{3,4}, Austin Greene^{1,7}, Laurie Raymundo⁸, Jen Dryden⁹, Audrey
7 Schlaff⁹, Jessica S Stella⁹, Tye L Kindinger¹⁰, Courtney S Couch^{11,10}, Douglas Fenner¹²,
8 Whitney Hoot¹³, Derek Manzello³, and Megan J Donahue¹.

9 1. Hawai‘i Institute of Marine Biology, Kāne‘ohe, HI, USA; jamie.sziklay@gmail.com

10 2. High Meadows Environmental Institute, Princeton University, Princeton, NJ, USA

11 3. NOAA/NESDIS/STAR Coral Reef Watch, 5830 University Research Court, College

12 Park, MD, USA

13 4. Global Science & Technology, Inc., 7501 Greenway Center Drive, Suite 1100, Greenbelt,

14 Maryland, USA

15 5. Physical Sciences and Marine Geophysics Laboratory, College of Science and

16 Engineering, James Cook University, Townsville, Queensland, Australia

17 6. Corals and Climate, USA

18 7. Woods Hole Oceanographic Institution, Woods Hole, USA

19 8. University of Guam Marine Laboratory, Mangilao, Guam, USA

20 9. Great Barrier Reef Marine Park Authority, Townsville, Queensland, Australia

21 10. Pacific Islands Fisheries Science Center, National Marine Fisheries Service, National
22 Oceanic and Atmospheric Administration, Honolulu, HI, USA
23 11. Cooperative Institute for Marine and Atmospheric Research, University of Hawai‘i at
24 Mānoa, Honolulu, HI, USA
25 12. Lynker Technologies, LLC, Contractor, NOAA Fisheries Service, Pacific Islands
26 Regional Office, Honolulu, HI USA
27 13. Guam Coral Reef Initiative, Government of Guam, Hagatña, Guam, USA
28 *Contact and corresponding author

29 **Keywords**

30 Coral reefs, disease, ecological forecasting, machine learning, quantile regression forests
31 **Open research statement:** Data are already published and publicly available, with those items
32 properly cited in this submission. All code used to create the disease models are available at:
33 https://github.com/jms5151/Fore-C_v2/tree/main/Fore-C_v2/codes. All code and data used to
34 create the weekly prediction updates are available at: <https://github.com/jms5151/Fore->
35 [C_v2/operational](https://github.com/jms5151/Fore-C_v2/tree/main/Fore-C_v2/operational). All code and data used to create the data explorer are
36 available at <https://github.com/jms5151/uh-noaa-shiny-app>. NOAA NCRMP fish survey data:
37 <https://www.fisheries.noaa.gov/inport/item/28844>;
38 <https://www.fisheries.noaa.gov/inport/item/34515>. NOAA NCRMP benthic survey data:
39 <https://doi.org/10.7289/v53n21q5>, <https://doi.org/10.7289/v579431k>,
40 <https://doi.org/10.7289/v5c24trh>, <https://doi.org/10.7289/v5zw1j8b>. Upon acceptance, all
41 underlying data and code pertinent to the results presented in the publication will be provided via
42 Zenodo.

43 Abstract

44 Ecological forecasts are becoming increasingly valuable tools for conservation and management.

45 However, there are few examples of near real-time forecasting systems that account for the wide

46 range of ecological complexities. We developed a new coral disease ecological forecasting

47 system that explores a suite of ecological relationships and their uncertainty and investigates how

48 forecast skill changes with shorter lead times. The Multi-Factor Coral Disease Risk product

49 introduced here uses a combination of ecological and marine environmental conditions to predict

50 risk of white syndromes and growth anomalies across reefs in the central and western Pacific and

51 along the east coast of Australia and is available through the U.S. National Oceanic and

52 Atmospheric Administration Coral Reef Watch program. This product produces weekly forecasts

53 for a moving window of six months at ~5 km resolution based on quantile regression forests. The

54 forecasts show superior skill at predicting disease risk on withheld survey data from 2012-2020

55 compared with predecessor forecast systems, with the biggest improvements shown for

56 predicting disease risk at mid- to high-disease levels. Most of the prediction uncertainty arises

57 from model uncertainty and therefore prediction accuracy and precision do not improve

58 substantially with shorter lead times. This result arises because many predictor variables cannot

59 be accurately forecasted, which is a common challenge across ecosystems. Weekly forecasts and

60 scenarios can be explored through an online decision support tool and data explorer, co-

61 developed with end-user groups to improve use and understanding of ecological forecasts. The

62 models provide near real-time disease risk assessments and allow users to refine predictions and

63 assess intervention scenarios. This work advances the field of ecological forecasting with real

64 world complexities, and in doing so, better supports near term decision making for coral reef

65 ecosystem managers and stakeholders. Secondarily, we identify clear needs and provide
66 recommendations to further enhance our ability to forecast coral disease risk.

67

68 **Introduction**

69 Forecasting coral disease outbreaks is critical for the timely management of reef
70 ecosystems, but developing such early warning systems is challenging when disease dynamics
71 are not well understood, and data are sparse and irregularly updated. Coral reefs and their
72 associated threats are a prime example of a complex system that presents challenges for
73 ecological forecasting. Coral reefs are dynamic, heterogeneous environments, characterized by
74 their diversity of species and species interactions, and physical and chemical factors that can
75 affect their health. Diseases are a major threat to coral reefs, causing up to 95% mortality in
76 dominant coral species during outbreak events such as the white band disease epidemic in the
77 1980s and 1990s and the Stony Coral Tissue Loss Disease outbreak in the 2010s and 2020s in
78 Florida and the Caribbean (Aronson and Precht 2001; Walton et al. 2018; Rosales et al. 2020).
79 Thus, innovative approaches to support effective management strategies for coral disease
80 transmission, prevention, and mitigation are urgently needed. Modern forecasting can now
81 combine mechanistic understanding, statistical and machine learning models, and the
82 quantification of uncertainty to make more accurate predictions. However, developing accurate
83 and reliable forecasts requires overcoming several key challenges, including the sparse
84 availability of high-quality data and limited understanding of the underlying complexity of
85 biological and environmental drivers of coral disease outcomes.

86 Developing early warning systems for coral diseases is a relatively recent endeavor that
87 aims to help managers and decision-makers take preventative actions and mitigative measures.

88 Given the widespread consensus linking coral disease to thermal condition (Burke et al. 2023),
89 early disease forecasts focused on using temperature to predict suitable conditions for disease.
90 The U.S. National Oceanic and Atmospheric Administration Coral Reef Watch (NOAA CRW)
91 program developed the first coral disease forecast in 2010 for white syndromes on the Great
92 Barrier Reef (GBR) in Australia (hereafter V1), which uses a decision tree framework based on a
93 series of anomalous thermal metrics (Heron et al., 2010). This system leveraged NOAA CRW's
94 established satellite sea surface temperature (SST) monitoring data (~50 km resolution, twice-
95 weekly) refining previous information about the relationship between thermal condition and
96 disease (Bruno et al., 2007; Selig et al., 2006). Subsequently, NOAA CRW adapted the thermal
97 condition metrics from the GBR to produce a complementary, experimental predictive tool for
98 coral disease in the Hawaiian archipelago (incorporated into V1). V1 was further developed to
99 incorporate finer resolution (~5 km, daily) SST data (hereafter V2). A retrospective analysis of
100 V2 demonstrated that machine learning algorithms that used the product metrics (i.e., summer
101 Hot Snaps) combined with additional biotic data could robustly reproduce disease prevalence
102 patterns for two coral diseases across three host species (Caldwell, Heron, et al., 2016). The
103 ability to nowcast and forecast some of these reef stressors has led to new and innovative
104 conservation practices and provided clarity to managers seeking to set priorities. While we know
105 of no examples yet where management officials have taken action in response to disease
106 forecasts, we have seen responses to NOAA CRW bleaching forecasts (Raymundo et al., 2022)
107 and we expect complementary actions (Beeden et al., 2012; Neely et al., 2021) will be taken in
108 response to disease forecasts as managers become more familiar with the system. Managers
109 could mitigate disease risk and impacts with a variety of local scale actions such as
110 implementing fishing and fishing gear restrictions, reducing land-based pollution runoff, or

111 reducing the abundance of known disease vectors (eg., corallivorous gastropods) or predators
112 (e.g., *Acanthaster planci*) from vulnerable reefs. Other experimental approaches could be
113 effective, including probiotics, phage therapy, or temporarily relocating at-risk colonies to
114 aquaria.

115 Moving beyond thermal conditions, the next generation of coral disease early warning
116 systems needs to better incorporate an expanded suite of conditions known or hypothesized to
117 affect disease dynamics. Previous research has statistically linked a range of conditions with
118 impaired coral health, including colony size and density, thermal condition, water quality, human
119 population density and land use, and fish densities and predation (Aeby, Williams, Franklin,
120 Haapkyla, et al., 2011; Aeby, Williams, Franklin, Kenyon, et al., 2011; Bruno et al., 2003;
121 Caldwell et al., 2020; Carlson et al., 2019; Greene et al., 2020; Haapkylä et al., 2011; Pollock et
122 al., 2014; Redding et al., 2013; Renzi et al., 2022). However, the mechanistic underpinnings of
123 these multiple contributing factors are often poorly understood due to their complex and non-
124 linear behavior, which can vary by host species and disease type (Clemens & Brandt, 2015;
125 Shore & Caldwell, 2019; Vega Thurber et al., 2014). An additional challenge for any early
126 warning system is whether the predictor variables themselves can be forecasted (Clark et al.,
127 2001; Oliver & Roy, 2015), and this is especially true for the diverse drivers of coral disease.
128 These challenges must be addressed to incorporate a wider range of putative disease drivers into
129 forecasting models.

130 Over the last decade, ecological forecasting and monitoring tools have advanced
131 considerably, making it possible to integrate multiple data streams and more robustly consider
132 various scenarios and sources of uncertainty (Clark et al., 2001; Dietze et al., 2018). Machine
133 learning algorithms are particularly useful in this context, as they can identify complex non-

134 linear relationships between variables and make predictions in data-poor environments (Jordan &
135 Mitchell, 2015). These advancements have enhanced the capability of identifying relationships
136 that should be tested further, allowing incremental improvements in forecasting efforts (Dietze et
137 al., 2018). Exploring likely scenarios within a forecasting framework can help create more robust
138 approaches for managing ecosystems. Plausible scenarios with alternate conditions are
139 developed using a combination of scientific information and models, stakeholder input, and
140 expert opinion. Scenarios can then be used to explore the potential impacts of different
141 management strategies, account for additional spatial variation in predictor variables, and/or
142 refine predictions to a specific set of conditions. By incorporating scenarios into ecological
143 forecasts and management plans, managers and decision-makers can better understand the
144 potential outcomes of different decisions and identify strategies that are more likely to be
145 effective under a range of possible futures (Clark et al., 2001). These models also need to be
146 incorporated into easy-to-use tools for managers to test and compare different management
147 actions.

148 In this paper, we present the next-generation NOAA CRW coral disease forecasting
149 product (i.e., V3) that addresses some of these challenges and applies new, innovative
150 approaches to ecological forecasting. By integrating data from multiple sources and using
151 machine learning algorithms to identify patterns and make predictions, the system provides early
152 warnings of coral disease risk and could help managers and decision-makers take proactive
153 measures to protect reefs across much of the Pacific Ocean. This new Multi-Factor Coral Disease
154 Risk product expands the previous product in several ways through: 1) a broader geographic
155 scope; 2) consideration of two distinct groups of diseases; 3) inclusion of a suite of disease
156 drivers; 4) generation of weekly forecasts with up to three-month lead time; 5) provision of

157 measures of uncertainty; 6) consideration of multiple scenarios; and 7) capacity for users to
158 visualize forecasts and modify scenarios through an interactive online dashboard used to explore
159 management strategies. The results of this study have broader implications for making
160 predictions in other complex, data-poor systems and highlight the need for continued research
161 and innovation in the field of ecological forecasting.

162

163 **Methods**

164 The Multi-Factor Coral Disease Risk product (i.e., V3) is an experimental regional
165 product, currently providing ecological forecasts for multiple locations in the Pacific Ocean.
166 Areas include American Samoa, Guam and the Commonwealth of the Northern Mariana Islands
167 (CNMI), Australia's Great Barrier Reef (GBR), Hawaii, and the U.S. Pacific Remote Islands
168 Marine National Monument (PRIMNM, also called the Pacific Remote Island Area, PRIA)
169 encompassing seven islands and atolls: Baker, Howland, and Jarvis Island; Johnston, Wake, and
170 Palmyra Atolls; and Kingman Reef. In this product, we assess disease risk based on satellite
171 remotely-sensed, modeled, and *in situ* data to provide nowcasts and near-term forecasts based on
172 current conditions, recent conditions, and subseasonal-to-seasonal forecasts from NOAA
173 operational climate models. We defined disease risk separately as a density (number of diseased
174 colonies/75m² ranging from 0 to infinity) in Australia and as a prevalence (percent of colonies
175 affected ranging from 0 to 100%) in the U.S. Pacific (more details below), which maps to
176 different NOAA CRW warning levels ranging from Low Risk to Alert Level 2 for visualization
177 purposes in the decision support tool. We determined the thresholds separating warning levels
178 based on historical disease observations and expert elicitation; the thresholds vary by disease

179 type and region (Appendix S1: Table S1). We optimized the modeling system using a Pacific-
180 wide dataset of over 42,000 coral disease surveys (more detail below).

181

182 **Data**

183 We identified a suite of potential predictor variables to forecast coral disease risk based
184 on prior observational, experimental, and modeling efforts for two disease types: white
185 syndromes and growth anomalies (Table 1, Appendix S1: Table S2).. White syndromes refer to a
186 suite of tissue loss diseases that cause coral mortality and range from acute to chronic based on
187 the speed at which the infection progresses (Bourne et al., 2015). Growth anomalies are chronic
188 diseases that persist at low levels year round and manifest as changes in skeletal morphology,
189 usually through abnormal increases in skeleton secretion and disorganization of corallites,
190 affecting colony growth and fecundity (Palmer & Baird, 2018). The etiological agents of both
191 groups of diseases are unknown. Across a variety of host species, disease types, and regions,
192 some factors such as coral cover, coral colony size, and specific ranges of temperature have been
193 consistently associated with certain coral diseases, although the functional relationships may
194 differ slightly (Bruno et al., 2007; Caldwell et al., 2020; Greene et al., 2020; Heron et al., 2010;
195 Ruiz-Moreno et al., 2012). Thus, we considered appropriate derivations of these variables for all
196 diseases and regions, based on data availability. For instance, we considered accumulation of
197 anomalous temperatures for white syndromes because of statistical associations across multiple
198 large scale studies (Bruno et al., 2007; Burke et al., 2023; Heron et al., 2010; Howells et al.,
199 2020; Maynard et al., 2011), but focused on seasonal mean temperature for growth anomalies
200 because it has been experimentally associated with lesion development and growth (Stimson,
201 2011). Additionally, there were several potential predictor variables that were unique to each

202 disease type, because the ecologies of white syndromes and growth anomalies differ
203 substantially. White syndromes often exhibit strong seasonality due to ocean conditions, notably
204 winter and summertime thermal stress and changes in water quality (Haapkylä et al., 2011;
205 Heron et al., 2010; Maynard et al., 2011; Ruiz-Moreno et al., 2012). White syndromes have also
206 been associated with fish densities, but the effects are not consistent across studies and the
207 underlying hypothesis for this effect varies by fish functional group (Aeby, Williams, Franklin,
208 Kenyon, et al., 2011; Caldwell et al., 2020; Clemens & Brandt, 2015; Greene et al., 2020; Renzi
209 et al., 2022; Williams et al., 2010). Thus, we included available metrics of fish density for
210 multiple fish types and water quality (turbidity) in the white syndromes models. For growth
211 anomalies, previous studies indicate an association with low fish abundance, limited water
212 motion, and poor water quality via nutrient enrichment, coastal development, and proximity to
213 dense human populations (Aeby, Williams, Franklin, Haapkyla, et al., 2011; Caldwell et al.,
214 2020; Yoshioka et al., 2016). Therefore, we included metrics of fish populations, turbidity, and
215 coastal development in the growth anomalies models.

216 From a forecasting perspective, the predictor variables, or environmental conditions, that
217 we considered in this study can be roughly divided into three types based on their variabilities
218 through time: 1) time-invariant; 2) seasonally-changing; and 3) regularly-changing. We consider
219 time-invariant conditions as any predictor variable that does not change regularly through time,
220 or information about such change is unavailable or sparsely updated. We consider seasonally-
221 changing conditions as predictor variables that depend on time of year but are not date-specific.
222 Most of these variables have been developed in a way that represents repeated seasonal patterns
223 developed from multi-year datasets (i.e., climatologies). Finally, we consider regularly-changing
224 conditions as predictor variables that change, and can be measured and evaluated, over some

225 regular time interval. We used point estimate predictor variable data for model development
226 based on the time and location of coral disease surveys whereas we use gridded predictor
227 variable data for forecasts.

228

229 *Time-invariant data*

230 We collated time-invariant data from *in situ* surveys and remotely-sensed data. For each
231 predictor variable described below, which we used in at least one of the four region-by-disease
232 models, we provide further detail, including data sources and spatial resolution, in Appendix 1:
233 Table S2. To characterize benthic cover, we used metrics of coral cover (0-100%), coral colony
234 size, and population level colony size variability (based on coefficient of variation). For these
235 metrics, we developed the models using data collected concurrently with coral disease surveys.
236 We aggregated these metrics by host family for both U.S. Pacific models and by morphology for
237 the GBR white syndromes models to be consistent with data collection methodology (more
238 details below). In the forecasts, we used a combination of survey data and gridded data from
239 long-term monitoring programs. For coral cover in the GBR and coral colony size in the U.S.
240 Pacific, we calculated ~5 km pixel-specific mean values across the reef grid from long-term
241 survey data (multiple sources listed in Appendix 1: Table S3) while for coral cover in the U.S.
242 Pacific, we used sector level benthic cover data from the NOAA National Coral Reef Monitoring
243 Program (NCRMP). As fish surveys were rarely conducted in coordination with benthic surveys,
244 we used fish density layers from long-term monitoring programs for both model development
245 and forecasting. We used sector-level fish data from NOAA NCRMP and ~2 km gridded fish
246 count data based on manta tow surveys from the Australian Institute of Marine Science (AIMS)
247 Long Term Monitoring Program (LTMP) (Sweatman et al., 2008). These long-term datasets

248 represent the most comprehensive current estimates of coral cover and size available for the reef
249 grid, but inherently will not contain information about recent or future changes in these variables.
250 Thus, periodic updates to the reef grid as data becomes available would be beneficial. As a proxy
251 for coastal development in both model development and forecasting, we used NASA's Black
252 Marble product, which is a time-aggregated map of artificial light intensity (high gain) (range =
253 0-255 where 0 = black and 255 = white) at 3 km resolution from the Visible Infrared Imaging
254 Radiometer Suite (VIIRS) instrument aboard the Suomi-National Polar-orbiting Partnership
255 (NPP) satellite (Román et al., 2018). To characterize chronic water quality conditions in both
256 model development and forecasting, we aggregated the diffuse attenuation coefficient at 490 nm,
257 $K_d(490)$, as a proxy for turbidity from VIIRS data (Kirk, 1994). We calculated long-term
258 $K_d(490)$ median and variability for each reef pixel by overlaying aggregated data from 2012-
259 2020 (i.e., all data available at the time of study) within a 5-pixel buffer (750 m becomes ~8.25
260 km resolution) following methods from Geiger et al., 2021 to increase data availability, as
261 nearshore ocean color data are notoriously patchy. These metrics are indicative of spatial
262 differences in water quality across reefs, providing information on locations that have
263 chronically good or poor water quality and those that are exposed to a large range of water
264 quality conditions throughout the year versus those with more consistent conditions.

265

266 *Seasonally-changing data*

267 We use month of year and two turbidity metrics (mean and variability) to capture
268 seasonally-changing conditions that are relevant to disease risk. To characterize typical seasonal
269 water quality patterns, we calculated mean and variability of VIIRS-derived $K_d(490)$ for a three-
270 week moving window (resulting in new values each week) across a 9-year time span (2012-

271 2020) using the same 5-pixel buffer described above. These metrics repeat annually and are
272 indicative of how water quality changes throughout the year at a given location. We used the
273 mean (i.e., climatology) and associated variability in Kd(490) to represent seasonal changes
274 because, to date, these values are too highly variable and too infrequently available in the coastal
275 zone to use actual, or even three-week composite, values. Additional details on the derivation of
276 these metrics and their accuracy can be found in Geiger et al., 2021. We include month in the
277 model as a proxy for all other seasonally changing conditions.

278

279 *Regularly-changing data*

280 We include three temperature-based metrics in the disease models that update at regular
281 intervals: 90-day SST mean, Hot Snap, and Winter Condition. In contrast to the seasonally-
282 changing data, the regularly changing data yield different values each year for the same time
283 period (e.g., the first week of January) based on observed and/or forecasted conditions. The daily
284 previous 90-day mean SST is the average daily SST values for the 90 days preceding the current
285 date. The Hot Snap and Winter Condition metrics were developed for NOAA CRW's Coral
286 Disease Outbreak Risk Product V1 and V2 and continue to be used in V3 to represent thermal
287 conditions on time scales relevant to coral disease. The Hot Snap metric accumulates hot
288 temperature anomalies through time, relative to the locally/pixel-specific long-term expected
289 summer season temperature (summer season climatology) (Heron et al., 2010), providing an
290 indication of exposure to thermal stress. The Winter Condition metric accumulates both hot and
291 cold temperature anomalies during the winter season relative to locally-specific, long-term
292 average temperature (Heron et al., 2010), representing cold season variability. Mild winters have

293 been linked to white syndromes (Caldwell, Heron, et al., 2016; Heron et al., 2010), potentially
294 because such conditions allow pathogens to persist and grow throughout the winter season.

295 The data underlying these three temperature metrics differ for satellite observed
296 temperatures, which we used for model development and near real-time nowcasts, and forecasted
297 temperature, which we use for disease forecasts. For observed SST, we use CoralTemp v3.1
298 (Skirving et al., 2020), which provides daily data at a global resolution of ~5 km (0.05°). For
299 forecasted SST, we use output from the NOAA National Centers for Environmental Prediction's
300 operational Climate Forecast System Version 2 (CFSv2) (Saha et al., 2014). Each day, the
301 CFSv2 generates an ensemble of four SST forecasts out to 9 months at ~50 km (0.5°) resolution.
302 We use this output to form 28 ensemble member predictions each week (4 daily start times x 7
303 days) for each predicted temperature metric and to predict the metric for each future week up to
304 three months following the prediction date. The data are downscaled from ~50 km to ~5 km
305 using a nearest neighbor algorithm and then bias-corrected to match the 5 km satellite SST
306 measurements during the overlap between satellite observations and CFSv2 over the weekly time
307 period when the 28 ensemble members are collected. Because predicted values demonstrate
308 decreased variability with longer lead-times, predicted SST anomaly values for the metrics are
309 correspondingly adjusted to match the variability of the SST data.

310

311 *Coral Disease Survey Data*

312 We assembled a Pacific-wide coral health monitoring dataset, which we used to develop
313 region- and disease-specific predictive models of disease risk. In total, we assembled over 42,000
314 coral health monitoring surveys between 2012 and 2020. Data came from the NOAA NCRMP,
315 University of Guam, Hawaii Coral Disease Database (Caldwell, Burns, et al., 2016), and the

316 Great Barrier Reef Marine Park Authority (GBRMPA; referred to as Reef Authority in other
317 contexts) Reef Health and Impact Surveys (Beeden et al., 2014). The different survey protocols
318 used to collect these data have been described in detail previously (Beeden et al., 2014; Caldwell,
319 Burns, et al., 2016; Winston et al., 2020). For the research described in this paper, there are
320 notable methodological differences between surveys conducted in Australia and the U.S. Pacific;
321 therefore, we modeled disease risk in these two regions separately. Specifically, surveys in
322 Australia indicated morphology-specific disease density (i.e., number of diseased colonies in a
323 given area) while the U.S. Pacific surveys provided information to quantify family-specific
324 disease prevalence (i.e., percent of coral colonies affected by disease); therefore the risk
325 prediction is for disease density for Australia and disease prevalence in the U.S. Pacific. While
326 the U.S. Pacific models are technically generated at the family level (Acroporidae for white
327 syndromes and Poritidae for growth anomalies), in practice, the data predominantly describe
328 genus- or species-specific patterns with various genera/species represented in different regions
329 (Appendix 1: Table S4). We used these data to develop predictive models of disease risk (i.e.,
330 disease density or prevalence) rather than outbreak risk, which we believe is more appropriate as
331 the data arise from regular monitoring surveys rather than outbreak response surveys (outbreaks
332 defined in Raymundo et al., 2008). If multiple surveys were conducted in close proximity in time
333 (i.e., in the same month) and space (the same survey area), we randomly selected one of those
334 surveys to keep in the dataset to avoid artificially over-representing certain conditions.

335

336 *Balancing data with SMOTE*

337 To create disease models that produce reliable predictions of all levels of disease risk,
338 particularly of high disease levels, we used a synthetic sampling technique to balance the data

339 used in model development. The observational surveys available to create the disease models
340 were highly unbalanced, with the majority of surveys reporting zero or low levels of disease
341 (Appendix 1: Table S5); using unbalanced data would optimize disease-free predictions.
342 Therefore, we balanced the dataset before model creation using the Synthetic Minority Over-
343 sampling Technique (SMOTE; Chawla et al., 2002; Fig. 1A). We used the observed disease
344 surveys with their associated predictor variables to create additional synthetic disease surveys
345 (using a k-nearest neighbor algorithm) to produce a balanced dataset (e.g., approximately equal
346 number of disease and disease-free surveys with all predictor variables). We created multiple
347 SMOTE datasets for each disease and region based on different disease level thresholds because
348 it is unknown whether the same environmental conditions that precede observed disease are
349 responsible for low and high levels of disease risk. In other words, we oversampled surveys with
350 any disease and oversampled surveys with greater than some specified level of disease allowing
351 the model selection process to determine the best threshold to use. We tested several disease
352 level thresholds: 1, 5, and 10 colonies/75m² for white syndromes in the GBR and 1, 5, and 10%
353 prevalence for white syndromes in the U.S. Pacific; 1, 5, 10, and 15 colonies/75m² for growth
354 anomalies in the GBR and 1, 5, 10, 15, and 20% prevalence for growth anomalies in the U.S.
355 Pacific. We chose these thresholds based on a combination of natural breaks in the data and
356 expert opinion. The threshold units align with the survey data collected (i.e., density or
357 prevalence) and therefore differ between the GBR and U.S. Pacific. For each SMOTE dataset of
358 disease surveys, we split the data into training and test data using a 75/25 split. We used the
359 training data for model creation and then the withheld test data for model selection and
360 assessment (described below).

361

362 *Quantile regression forests*

363 We created predictive models of disease risk using quantile regression forests
364 (Meinshausen, 2006; Fig. 1B). Quantile regression forests use a decision tree framework, allow
365 for non-linear relationships between response and predictor variables, and have shown high
366 predictive skill across a range of systems. Briefly, quantile regression forests are created by
367 developing an ensemble of quantile decision trees (i.e., random forests), with each tree created
368 from a bootstrapped resample of the dataset. Quantile decision trees differ from standard
369 decision trees in that they predict the distribution of target values rather than the mean target
370 value from the training data. This approach uses an ensemble of uncorrelated decision trees,
371 which tend to outperform any individual tree, and each tree uses a random subset of predictors to
372 increase variation among trees. The result of this process is that the final predictive model is
373 more robust because it is created from many trees that are trained on different subsets of
374 response data and predictor variables.

375

376 *Model selection*

377 We selected the most parsimonious model for each disease and region amongst a suite of
378 candidate models based on predictive skill on a withheld portion of the data. For each disease-
379 by-region pair, we ran a model that included all hypothesized predictor variables (Table 1) from
380 a training dataset (75% of surveys) and then used a backward selection approach to iteratively
381 remove predictor variables of least importance. We calculated the relative importance of each
382 predictor variable as the percent increase in Mean Squared Error (MSE) of out-of-bag cross-
383 validation predictions across permutations in that predictor variable, with higher values
384 indicating more important predictor variables. The exception was for the predictor variable

385 Month, which we retained in the model regardless of its relative importance because it captures
386 additional seasonal variation. At each model iteration, we predicted disease risk from a withheld
387 test dataset (25% of the surveys) and assessed predictive skill based on the R^2 value that arose
388 from linearly regressing those predictions with observations. We followed this approach of
389 backward selection for each SMOTE dataset. The selected (most parsimonious) model was the
390 model with the fewest predictor variables that produced an R^2 value within 1% of the best model
391 (i.e., model with the highest R^2 overall).

392

393 *Model assessment*

394 To determine how well the models performed at retrospectively predicting disease risk
395 for each disease-by-region pair, we compared retrospective predictions by the models described
396 here with archived nowcasts from previous versions of the models where available (i.e., V2
397 predictions for the GBR and Hawaiian archipelago) and how forecast skill changes with different
398 lead times. For both assessments, we quantified predictive skill using the withheld test data. To
399 assess predictive skill for white syndromes, we compared retrospective disease predictions from
400 models described in this paper (V3) with models supporting V2 using predictor data available
401 from the corresponding week of observations. The V3 models predict disease density or
402 prevalence whereas the V2 models produce risk levels based on Hot Snap values (units = $^{\circ}\text{C}$ -
403 weeks, range = 1-15); therefore, we visually compared these results but did not directly compare
404 their skill quantitatively. Since there are no previous models in production for growth anomalies,
405 we assessed the retrospective model skill on the withheld test data alone. Additionally, we were
406 interested in whether and to what extent forecast prediction accuracy and precision change as we
407 get closer to the observation date (i.e., shorter lead-times). To assess this relationship, we

408 predicted disease risk at weekly intervals for each observation date in the withheld data, with
409 lead times ranging from 12 weeks prior (e.g., in advance of a survey) to 0 weeks (i.e., nowcast).
410 We calculated accuracy as the difference between the 75th quantile prediction and the
411 observation, resulting in zero if there was perfect accuracy, negative values if the models
412 predicted lower disease risk than observed, and positive values if the models predicted higher
413 disease risk than observed. We used the 75th quantile prediction (upper range of disease
414 likelihood) as the primary indicator of disease risk throughout this work, which was the metric
415 selected by the product end users to err on the side of potentially overpredicting disease in an
416 effort to further capture rare disease events. To assess predictive precision, we calculated the
417 difference between the 90th and 50th quantile predictions: larger differences indicate less precise
418 estimates and smaller differences indicate more precise estimates.

419

420 *Weekly-updating predictions*

421 The overarching objective of this research was to develop a product that provides
422 weekly-updated, near real-time, and subseasonal-to-seasonal disease risk forecasts. The
423 workflow for this process follows. First, we developed a reef location database based on a ~5 km
424 gridded reef locations dataset currently used by NOAA CRW (Heron et al., 2016) to set the
425 spatial extent of the disease risk forecasts described in this paper. This reef location database
426 encompasses all known shallow-water reefs within the U.S. Pacific Islands and atolls and along
427 the east coast of Australia, the majority of which fall within the GBR Marine Park. To allow
428 users to assess short-term temporal evolution of disease risk at each reef pixel, we provide a
429 moving window of six months of weekly predictions: the first three months with weekly nowcast
430 predictions based on observed environmental conditions (i.e., time-invariant, seasonally-

431 changing, and nowcast predictor variables identified in the model selection process described
432 above) up to the current calendar week, and the second three months with weekly forecast
433 predictions based on a combination of historically observed (time-invariant data and seasonally-
434 changing data) and forecasted environmental conditions. The models and environmental
435 conditions we use vary by disease and region, as described earlier and in the Results section. For
436 each week of predictions, we update the environmental input data (Fig. 1C). The nowcast
437 predictions (Fig. 1D) that we produce for each reef pixel are based on a single set of observed
438 environmental conditions and prediction uncertainty arises solely due to model uncertainty. In
439 contrast, we produce 28 ensemble forecast predictions for each reef pixel (Fig. 1D), using 28 sets
440 of SST-based metrics derived from the 28 different CFSv2 model runs, and thus, uncertainty is
441 composed of both model uncertainty and SST forecast uncertainty. In this product, we chose to
442 present predictions using the 50th, 75th, and 90th quantile predictions for the reasons stated
443 above (though any quantile(s) could be used). We also aggregate the risk predictions for different
444 management areas, which we collated from marine management agencies. We do this by
445 quantifying the 90th quantile values across all ~5 km reef pixels that fall within the specified
446 management area of the risk predictions (i.e., the 75th quantile modeled risk). The use of the
447 90th quantile to spatially summarize risk predictions is consistent with other regional summaries
448 produced by CRW (Heron et al., 2016), with this value selected to alert users to regional-level
449 risk whilst preventing potential exaggeration (e.g., by reporting the maximum value across the
450 region).

451

452 *Weekly-updated scenarios*

453 To allow users to customize the prediction to localized and current environmental

454 conditions and help determine the most appropriate intervention strategies, we also produce
455 weekly-updated scenario-based disease risk predictions (Fig. 1E). The predictions for various
456 scenarios show how adjusting current environmental conditions would change current disease
457 risk predictions. We calculate the change in disease risk by re-running the models iteratively,
458 varying a single environmental condition by specified amounts and holding all other location-
459 specific, current environmental conditions constant. The resulting scenarios allow users to 1)
460 refine predictions considering local conditions (e.g., a reef of interest) known to the user that
461 may vary from the mean conditions of the entire reef pixel or management zone; and 2) consider
462 how an intervention (e.g., a program to reduce turbidity) would affect disease risk. Following the
463 format we use to present near real-time and seasonal disease risk predictions, we also calculate
464 changes in disease risk for scenarios based on the 75th quantile disease predictions and aggregate
465 the results to management areas in the same way we describe earlier.

466

467 **Results**

468 *Performance evaluation*

469 The new Multi-Factor Coral Disease Risk product (V3) described in this study predicts
470 disease risk relatively well and qualitatively demonstrates superior predictive accuracy compared
471 with V2 for both the GBR and Hawaiian archipelago (Fig. 2). All versions have difficulty
472 predicting no or very low disease levels (i.e., below the selected SMOTE thresholds). V3 is the
473 first product to calculate uncertainty and can therefore represent this lack of predictability with
474 large uncertainty values, as shown around many low disease values. The major improvement can
475 be seen at mid- and high-levels of disease (i.e., above the selected SMOTE thresholds, which
476 vary by disease and region). While the previous algorithm predicted some high disease events

477 well, many were predicted to have no disease risk, suggesting that factors other than thermal
478 condition are key for predicting disease events.

479

480 *Lead time*

481 Both accuracy and precision improved as lead time decreased, but not as drastically and
482 consistently as we expected (Fig. 3), indicating that as the survey date approaches the predictions
483 improve slightly. Positive values for accuracy indicate an over-prediction of disease in the
484 forecast (as shown for white syndromes on the GBR), whilst negative values indicate under-
485 prediction (growth anomalies in both regions). Accuracy improved with shorter lead time for
486 predictions in the GBR for both diseases, while there was almost no improvement with lead time
487 for predictions in the U.S. Pacific. In contrast, precision was largely unaffected by lead time,
488 with marginal improvements for white syndromes in the GBR and growth anomalies in the U.S.
489 Pacific. Given that the variability in SST forecasts decreased with increasing lead time, these
490 results suggest that the prediction uncertainty is largely a function of model uncertainty rather
491 than SST forecast uncertainty.

492

493 *Coral disease drivers*

494 The most influential disease drivers were primarily time-invariant or seasonally-changing
495 predictor variables (Table 1), which may explain why the V3 product predicts disease with
496 relatively high accuracy for observations from a range of locations and years (Fig. 2), but those
497 predictions do not change substantially with changing lead-times (Fig. 3). The most
498 parsimonious models for each disease-by-region pair varied slightly from each other but broadly
499 reflected relationships found in the literature (Appendix 1: Figs. S1-4). In short, both diseases

500 were primarily influenced by temperature and water quality, coral cover or size, and fish density.
501 White syndromes were strongly influenced by seasonal conditions while growth anomalies were
502 more strongly driven by chronic conditions. A major contribution of this study is the inclusion of
503 multiple metrics of chronic and seasonally changing water quality, which have been shown to
504 influence disease risk in both small-scale correlative and experimental studies (Haapkylä et al.
505 2011; Pollock et al. 2014; Vega Thurber et al. 2014; Yoshioka et al. 2016), but to-date, have not
506 been possible to include in large scale studies. Thus, this research demonstrates a consistent
507 influence of water quality on disease risk across a broad geographic region and two disease
508 types. Fish density and winter condition were the best predictors of white syndromes in the GBR,
509 followed by variation in seasonal turbidity, summer thermal condition, and coral cover. For
510 white syndromes in the U.S. Pacific, median colony size and chronic and seasonal turbidity
511 metrics (both median and variability for each) were most important. Predictor variables for
512 growth anomalies in both regions were similar to each other, and included 90-day SST mean,
513 fish density, benthic cover metrics, and seasonal and chronic water quality. Within-site water
514 quality variability was more important for growth anomalies in the GBR, whereas average water
515 quality conditions along with coastal development were more important in the U.S. Pacific.

516 The model selection process revealed that the predictor variables used are better suited
517 for differentiating between lower and higher levels of disease risk rather than presence-absence.
518 We found that the models were able to predict the gradient of observed disease risk best when
519 oversampling surveys in the SMOTE balancing process with relatively high levels of disease
520 risk. For white syndromes, oversampling surveys with >10 diseased colonies/ 75m^2 in the GBR
521 and $>10\%$ disease prevalence in the U.S. Pacific was optimal; for growth anomalies,

522 oversampling surveys with >15 diseased colonies/75m² in the GBR and >20% disease
523 prevalence in the U.S. Pacific models was optimal (Appendix 1: Fig. S5).

524

525 *Decision support tools*

526 The experimental Multi-Factor Coral Disease Risk Forecast, a new tool within NOAA
527 CRW's decision support system for coral reef management, provides a regional ecological
528 nowcast and forecast of white syndromes and growth anomalies for multiple locations in the
529 Pacific Ocean. Via an online interface on the CRW website
530 (https://coralreefwatch.noaa.gov/product/disease_multifactor/index.php), users can access and
531 explore coral disease forecasts for their region of study, management, and/or interest in the
532 Pacific, to prepare for, monitor, and respond to elevated coral disease risk (Appendix 1: Fig. S6).

533

534 *Data explorer*

535 To allow users to explore near real-time, weekly, and seasonal disease predictions more
536 closely, we produced an interactive data explorer tool to complement the NOAA CRW Multi-
537 Factor Coral Disease Risk Forecast. Users can access the data explorer through
538 https://coralreefwatch.noaa.gov/product/disease_multifactor/index.php or at
539 <https://coraldisease.com>. The data explorer has four components: 1) a disease risk page
540 visualizing nowcasts and forecasts across time and space (Fig. 4); 2) a scenarios page where
541 users can adjust environmental conditions to assess corresponding changes in the nowcast of
542 spatially-explicit disease risk (Appendix S1: Fig. S7); 3) a historical data page that provides
543 information about survey data used to build the models; and 4) an information page with
544 explanatory information and additional resources. Users can explore forecasts and scenarios at

545 multiple spatial scales, ranging from an individual ~5 km reef pixel to various management
546 zones (containing multiple reef pixels).

547

548 **Discussion**

549 The Multi-Factor Coral Disease Risk product (V3) offers many improvements over its
550 predecessors, providing a more holistic assessment of disease risk for reefs throughout the
551 Pacific Ocean. In addition to expanding the geographic scope and types of diseases assessed, V3
552 provides weekly-updated nowcasts and forecasts with up to three months of lead time. The
553 predecessor products fundamentally differed in their forecasting approach; V1 and V2 provide
554 winter pre-conditioning risk outlooks at the end of winter based on wintertime metrics derived
555 from satellite remote sensing data, and then for pixels that are pre-conditioned for risk, refined
556 near real-time predictions are based on satellite monitoring of Hot Snap accumulation throughout
557 the summer months. Thus, within the summer, these prior products produce nowcasts and do not
558 make future predictions; the only prediction component is for the following summer and only at
559 the conclusion of a winter season based on thermal conditions from the entire winter.
560 Operationally, V3 requires constructing regular predictions of SST-based metrics from climate
561 models rather than relying entirely on near real-time satellite remote sensing (as in V1 and V2).
562 The three-month lead time in V3 aims to provide local stakeholders with more time to organize
563 and execute a response to potential elevated disease risk. The accuracy and precision of disease
564 risk forecasts demonstrate a marginal level of bias in applying the data-based model relationships
565 with predicted values, which may result from variable skill in predicting the inputs (which here
566 are the temperature-based metrics) rather than in the model itself (see further discussion below).
567 Through the online dashboard, users can vary current or predetermined environmental conditions

568 to refine disease risk predictions to better reflect local conditions within the data grid and/or to
569 assess impacts of potential interventions. The most fundamental difference between V1/V2 and
570 V3 is that the new product assesses disease risk based on a suite of ecological conditions in
571 combination with temperature conditions, rather than temperature alone. Some of these new
572 variables such as turbidity were previously unavailable before the incorporation of VIIRS data
573 into these models. Given the relative importance of these new predictor variables (Table 1), we
574 can conclude that although suitable temperature conditions are necessary for elevating risk of
575 white syndromes and growth anomalies, other conditions like colony size and water quality are
576 important driving factors. As a result, the new models that consider a suite of conditions,
577 alongside temperature, have demonstrated better performance in retrospectively predicting
578 disease risk in both the GBR and U.S. Pacific.

579 While this analysis demonstrates that a suite of conditions are associated with white
580 syndromes and growth anomalies, challenges in forecasting these predictor conditions directly
581 limits capacity for disease prediction. The only predictor variables that are truly forecasted in the
582 Multi-Factor Coral Disease Risk product are the SST-based metrics. For all other variables, we
583 created seasonal climatologies, or rely on time-invariant layers based on long-term aggregated
584 data. For most of the time-invariant variables, such as coral cover, fish densities, and coastal
585 development, we do not expect conditions to change regularly. However, a single event can
586 drastically change biotic conditions on a reef (e.g., a mass bleaching event) and such changes
587 would not be reflected in the forecasts with the predetermined conditions, although they may be
588 assessed (at least to some degree) through adjusting scenarios based on updated information. We
589 anticipate the data may be updatable every 5 to 10 years. We foresee a similar issue for water
590 quality metrics: while we expect that the seasonal climatology and associated variability metric

591 used in these models are fairly robust in the long-term, the current models do not capture acute
592 events caused by intense rainfall and associated runoff, which are known to influence disease
593 (Haapkylä et al., 2011). Although we attempted to measure acute events with ocean color data
594 (procedure described in Geiger et al., 2021), we found that the available data were too sparse to
595 use in the models, with no satellite coverage for ~80% of the corresponding survey data. More
596 importantly, the ocean color data unavailable during events were not random, but aggregated
597 during cloudy days; in other words, days that are most likely associated with rain events that can
598 increase disease risk. An alternative approach to forecasting water quality conditions could be to
599 create a model based on precipitation forecasts. However, precipitation forecasts are less skillful
600 than temperature forecasts and would require accurate prediction of the timing, intensity, and
601 location of rainfall at fine scales, which must be incorporated into fine-scale hydrologic models
602 with accurate topography and well-predicted initial surface conditions (i.e., soil moisture). Such
603 fine scale hydrologic modeling is generally lacking for most tropical coasts. For this reason,
604 seasonally varying water quality climatologies are the most reliable measurements currently
605 available for coastal coral reefs and applicable for our models. However, we see this process as
606 analogous to early temperature forecasts, which began as almanacs of past conditions
607 (climatologies) and now show high prediction skill through the deployment of increasingly
608 sophisticated statistical and dynamical models.

609 The extent to which temperature-based metrics are influential in the models determines
610 how well predictions reflect spatial and temporal variability in disease risk. For white syndromes
611 on the GBR for example, both Winter Condition and Hot Snaps are relatively influential
612 variables. As a result, in the retrospective analysis, accuracy and precision varied
613 spatiotemporally – and improved with shorter lead times (consistent with the performance of

614 predicted temperature). In contrast, white syndromes in the U.S. Pacific are less strongly driven
615 by any of the temperature metrics tested in this study, and therefore variability in disease risk is
616 more apparent spatially than temporally. It is worthwhile to note that several white syndromes
617 outbreaks in the U.S. Pacific have occurred in winter (Aeby et al., 2016; Caldwell et al., 2018;
618 Greene et al., 2023; Williams et al., 2011), suggesting that other factors may be more important
619 than temperature in this region and/or that some aspect of temperature not captured by the
620 metrics used in this study is important. For all disease-region pairs, particularly those with less
621 reliance on temperature-based metrics, developing and/or improving climatologies and forecast
622 variables other than temperature would be the most effective way to improve predictability
623 within this forecasting system. A complementary and useful way of leveraging information from
624 V3 is to explore the spatial variability in disease risk to identify locations that are most promising
625 for interventions to improve reef health and target interventions to the most influential variables.
626 For instance, for white syndromes on the GBR, fish density and seasonal turbidity variability
627 were identified as some of the most important predictor variables, indicating that interventions
628 directed at those factors may be most effective for improving reef health. From this perspective,
629 users can explore spatial variability in disease risk and then track any intervention-associated
630 improvements through time without concern over ephemeral conditions that will elapse with
631 weekly updating.

632 Ecological forecasting presents a variety of ways scientists, managers, and decision-
633 makers can address the rising number of ecological challenges. We provide multiple pathways to
634 explore model predictions and suggest that major improvements going forward will be as
635 dependent on understanding the biological relationships as they are on additional monitoring and
636 surveillance data. The model outputs and associated online Multi-Factor Coral Disease Risk

637 product and data explorer were co-developed with many relevant management agencies and
638 scientists. Through multiple focus groups with stakeholders in Australia, American Samoa,
639 Hawaii, and Guam, planning meetings, and workshop demonstrations at several scientific
640 conferences over the course of six years, we created an online decision support tool that provides
641 regional overviews aligned with other NOAA CRW tools with which our intended audience is
642 already familiar. The method of delivering regional overviews is also preferred by users with
643 slow or intermittent internet connection, as is common in some Pacific islands. The data explorer
644 complements this tool in several ways. First, it provides predictions aggregated to relevant
645 management zones and allows users to explore forecasts at these various spatial scales through
646 time. This addresses two key concerns of our users as they need to distill information at scales
647 relevant to their respective agencies or work mandates, and to understand trends through time in
648 those specific locations. We addressed a suite of other concerns through the use of scenarios.
649 Broadly, users who interacted with the tools as they were being developed and tested found it
650 difficult to translate mean conditions at the finest spatial scale (~5 km) available to an individual
651 reef of interest, especially when they knew conditions at that one location were different from the
652 surrounding region. Thus, we made it possible for users to change individual input conditions in
653 the scenarios page of the interactive tool to see how predicted disease risk may correspondingly
654 change in a specified area of interest. The same scenarios tool can alternatively be used as an
655 exercise to assess the predicted impacts of an intervention that would affect the relevant input
656 conditions (e.g., an intervention to reduce resuspended sediments via turbidity) to determine how
657 that might affect disease risk.

658 Going forward, the forecasting models could be substantially improved by replacing
659 phenomenological relationships with biological ones and potentially by calibrating the models

660 differently. Ideally, biological relationships could replace phenomenological ones by using a
661 combination of lab and natural experiments. This approach would ultimately help reduce
662 uncertainty, particularly for undersampled conditions. In terms of calibration, we made several
663 decisions that increased the likelihood of false positives (i.e., predicting higher disease levels
664 than would be observed). Specifically, using SMOTE to compensate for scarce data on the
665 conditions associated with elevated disease risk resulted in an overrepresentation of those
666 conditions in the model data. Further, we used the 75th percentile when communicating the
667 model results in an effort to guard against missing a major disease event. The impact of these
668 decisions plays out as expected with a large number of false positives in the validation exercise
669 (Fig. 2). While we made these choices based on stakeholder input, it might be preferable in
670 future work to calibrate the models in a way that systematically assesses a broader suite of
671 assumptions and allows for optimization of those decisions. For instance, future efforts might
672 include performing a formal parameter sweep across a broader range of SMOTE data
673 frequencies and prediction quantiles. Alternatively, if enough information is known about the
674 disease system, one could use informative priors in a Bayesian analysis or consider adding a base
675 rate correction.

676 The overall modeling approach we used to create V3 could be replicated to predict
677 disease risk for other reef regions and diseases, with appropriate consideration given to the
678 transferability of input variables to these model systems. To expand this framework, a model
679 would need to be developed tailored to the new location and/or disease. This would require the
680 collation of coral health survey data and concurrent environmental conditions for model
681 development, and collating gridded environmental covariates, including climatologies and SST
682 forecasts, for the appropriate reef grid for forecasting. Diseases most suited for a forecasting

683 framework like the one described in this study are those impacting widely distributed hosts,
684 where the burden shifts seasonally between endemic and epizootic states. For example, Stony
685 Coral Tissue Loss Disease has caused widespread mortality in multiple species in the Caribbean
686 and would be an ideal candidate disease for expanding the current framework if it were
687 introduced to the Pacific basin or through the expansion of this tool to the western Atlantic.

688 Many of the issues that make it challenging to forecast coral disease risk are issues that
689 encumber ecological forecasts more broadly. In many ecological systems, the greatest obstacle is
690 data limitation. For example, while we had extensive coral disease survey data that spanned a
691 large geographic range in the Pacific Ocean and a broad time horizon, very few of the data points
692 contained useful information about disease density or prevalence, as most surveys exhibited low
693 or disease-free conditions. This problem is likely to arise in other attempts to forecast low
694 occurrence events such as infestations, invasive species, tipping points, and extreme events.
695 While the historical low occurrence of disease is good ecologically, these data limitations inhibit
696 both our ability to develop initial ecological forecasts and to create a workflow with continual
697 validation and updates, which has been key to improving forecasts in other systems such as
698 weather, storm, and fire forecasting (Dietze et al., 2018). A complementary issue is the reliance
699 on forecasted data as inputs to an ecological forecasting model, which may have their own set of
700 uncertainties and challenges. An important question then arises from these shared obstacles
701 across systems: is there something inherently different and currently unknown about developing
702 forecasts in systems where data cannot be regularly updated and validated? Thus, this ecological
703 forecast and many others will benefit from community-wide progress in the field of ecological
704 forecasting.

705

706 **Conclusions**

707 Herein, we present the next-generation NOAA CRW coral disease forecasting product
708 and an associated data explorer tool. It provides many advantages over its predecessors,
709 including near-term forecasts of coral disease risk in many major reefs in the Pacific Ocean. The
710 Multi-Factor Coral Disease Risk product predicts disease risk for white syndromes and growth
711 anomalies with greater precision and accuracy than previous products based on temperature
712 alone, and provides information for more diseases and regions. Co-developing the user interface
713 with the intended user base of scientists and managers resulted in a user-friendly online data
714 explorer tool that includes assessment of disease risk at different scales, quantification of
715 uncertainty in predictions, and the ability to adjust input conditions to assess effects on disease
716 outcomes. While this iteration is a major improvement to the NOAA CRW coral disease
717 forecasting products, largely thanks to numerous advances in the ecological forecasting
718 community and data availability, there are still numerous limitations for forecasting coral disease
719 risk. As data availability, forecasting capabilities, and our biological understanding of the system
720 improves, so can future versions of this product.

721

722 **Acknowledgments:** Sincere thanks to Maury Estes of the NASA Ecological Forecasting
723 Program for guidance and support throughout the project. Thanks also to the numerous people
724 who provided feedback during the development of the tools through formal workshops, user-
725 engagement meetings, and/or personal input as well as constructive feedback from two
726 anonymous Reviewers. The scientific results and conclusions, as well as any views or opinions
727 expressed herein, are those of the authors and do not necessarily reflect the views of NOAA or
728 the Department of Commerce.

729

730 **Funding:** Version 3 (V3) product development was supported with funding from the NASA
731 Ecological Forecasting Program (Applied Sciences Program), through the University of Hawai'i-
732 Hawai'i Institute of Marine Biology, with support to NOAA Coral Reef Watch via Global
733 Science & Technology, Inc. It was conducted in close collaboration with James Cook University,
734 the University of Newcastle, and the University of New South Wales, through the multi-year
735 Fore-C project, "Forecasting Coral disease outbreaks across the tropical Pacific Ocean using
736 satellite-derived data". We thank the NOAA Coral Reef Conservation Program, which funds
737 Coral Reef Watch (CRW; CRCP Project #915) and the National Coral Reef Monitoring Program
738 (NCRMP project # 743; CRCPP); NCRMP was the source of the benthic and fish data in the
739 Pacific.

740 **Conflicts of interest:** On behalf of all authors, the corresponding author states that there is no
741 conflict of interest.

742

743

744

745

746

747

748

749

750

751 **Literature Cited**

752 Aeby, G. S., Callahan, S., Cox, E. F., Runyon, C., Smith, A., Stanton, F. G., Ushijima, B., &
753 Work, T. M. (2016). Emerging coral diseases in Kāne‘ohe Bay, O‘ahu, Hawai‘i (USA): two
754 major disease outbreaks of acute Montipora white syndrome. *Diseases of Aquatic
755 Organisms*, 119(3), 189–198.

756 Aeby, G. S., Williams, G. J., Franklin, E. C., Haapkyla, J., Harvell, C. D., Neale, S., Page, C. A.,
757 Raymundo, L., Vargas-Ángel, B., Willis, B. L., Work, T. M., & Davy, S. K. (2011). Growth
758 anomalies on the coral genera Acropora and Porites are strongly associated with host density
759 and human population size across the Indo-Pacific. *PLoS One*, 6(2), e16887.

760 Aeby, G. S., Williams, G. J., Franklin, E. C., Kenyon, J., Cox, E. F., Coles, S., & Work, T. M.
761 (2011). Patterns of coral disease across the Hawaiian archipelago: relating disease to
762 environment. *PLoS One*, 6(5), e20370.

763 Beeden, R. J., Turner, M. A., Dryden, J., Merida, F., Goudkamp, K., Malone, C., Marshall, P. A.,
764 Birtles, A., & Maynard, J. A. (2014). Rapid survey protocol that provides dynamic
765 information on reef condition to managers of the Great Barrier Reef. *Environmental
766 Monitoring and Assessment*, 186(12), 8527–8540.

767 Beeden, R., Maynard, J. A., Marshall, P. A., Heron, S. F., & Willis, B. L. (2012). A framework
768 for responding to coral disease outbreaks that facilitates adaptive management.
769 *Environmental Management*, 49(1), 1–13.

770 Bourne, D. G., Ainsworth, T. D., Pollock, F. J., & Willis, B. L. (2015). Towards a better
771 understanding of white syndromes and their causes on Indo-Pacific coral reefs. *Coral Reefs* ,
772 34(1), 233–242.

773 Bruno, J. F., Petes, L. E., Drew Harvell, C., & Hettinger, A. (2003). Nutrient enrichment can

774 increase the severity of coral diseases. *Ecology Letters*, 6(12), 1056–1061.

775 Bruno, J. F., Selig, E. R., Casey, K. S., Page, C. A., Willis, B. L., Harvell, C. D., Sweatman, H.,
776 & Melendy, A. M. (2007). Thermal stress and coral cover as drivers of coral disease
777 outbreaks. *PLoS Biology*, 5(6), e124.

778 Burke, S., Pottier, P., Lagisz, M., Macartney, E. L., Ainsworth, T., Drobniak, S. M., &
779 Nakagawa, S. (2023). The impact of rising temperatures on the prevalence of coral diseases
780 and its predictability: A global meta-analysis. *Ecology Letters*.
781 <https://doi.org/10.1111/ele.14266>

782 Caldwell, J. M., Aeby, G., Heron, S. F., & Donahue, M. J. (2020). Case-control design identifies
783 ecological drivers of endemic coral diseases. *Scientific Reports*, 10(1), 2831.

784 Caldwell, J. M., Burns, J. H. R., Couch, C., Ross, M., Runyon, C., Takabayashi, M., Vargas-
785 Ángel, B., Walsh, W., Walton, M., White, D., Williams, G., & Heron, S. F. (2016). Hawai‘i
786 Coral Disease database (HICORDIS): species-specific coral health data from across the
787 Hawaiian archipelago. *Data in Brief*, 8, 1054–1058.

788 Caldwell, J. M., Donahue, M. J., & Harvell, C. D. (2018). Host size and proximity to diseased
789 neighbours drive the spread of a coral disease outbreak in Hawai‘i. *Proceedings. Biological
790 Sciences / The Royal Society*, 285(1870). <https://doi.org/10.1098/rspb.2017.2265>

791 Caldwell, J. M., Heron, S. F., Eakin, C. M., & Donahue, M. J. (2016). Satellite SST-Based Coral
792 Disease Outbreak Predictions for the Hawaiian Archipelago. *Remote Sensing*, 8(2), 93.

793 Carlson, R. R., Foo, S. A., & Asner, G. P. (2019). Land Use Impacts on Coral Reef Health: A
794 Ridge-to-Reef Perspective. *Frontiers in Marine Science*, 6.
795 <https://doi.org/10.3389/fmars.2019.00562>

796 Chawla, N. V., Bowyer, K. W., Hall, L. O., & Kegelmeyer, W. P. (2002). SMOTE: Synthetic

797 Minority Over-sampling Technique. *Journal of Artificial Intelligence Research*, 16, 321–

798 357.

799 Clark, J. S., Carpenter, S. R., Barber, M., Collins, S., Dobson, A., Foley, J. A., Lodge, D. M.,

800 Pascual, M., Pielke, R., Jr, Pizer, W., Pringle, C., Reid, W. V., Rose, K. A., Sala, O.,

801 Schlesinger, W. H., Wall, D. H., & Wear, D. (2001). Ecological forecasts: an emerging

802 imperative. *Science*, 293(5530), 657–660.

803 Clemens, E., & Brandt, M. E. (2015). Multiple mechanisms of transmission of the Caribbean

804 coral disease white plague. *Coral Reefs* , 34(4), 1179–1188.

805 Dietze, M. C., Fox, A., Beck-Johnson, L. M., Betancourt, J. L., Hooten, M. B., Jarnevich, C. S.,

806 Keitt, T. H., Kenney, M. A., Laney, C. M., Larsen, L. G., Loescher, H. W., Lunch, C. K.,

807 Pijanowski, B. C., Randerson, J. T., Read, E. K., Tredennick, A. T., Vargas, R., Weathers,

808 K. C., & White, E. P. (2018). Iterative near-term ecological forecasting: Needs,

809 opportunities, and challenges. *Proceedings of the National Academy of Sciences of the*

810 *United States of America*, 115(7), 1424–1432.

811 Geiger, E. F., Heron, S. F., Hernández, W. J., Caldwell, J. M., Falinski, K., Callender, T.,

812 Greene, A. L., Liu, G., De La Cour, J. L., Armstrong, R. A., Donahue, M. J., & Eakin, C. M.

813 (2021). Optimal Spatiotemporal Scales to Aggregate Satellite Ocean Color Data for

814 Nearshore Reefs and Tropical Coastal Waters: Two Case Studies. *Frontiers in Marine*

815 *Science*, 8. <https://doi.org/10.3389/fmars.2021.643302>

816 Greene, A., Donahue, M. J., Caldwell, J. M., Heron, S. F., Geiger, E., & Raymundo, L. J. (2020).

817 Coral Disease Time Series Highlight Size-Dependent Risk and Other Drivers of White

818 Syndrome in a Multi-Species Model. *Frontiers in Marine Science*, 7.

819 <https://doi.org/10.3389/fmars.2020.601469>

820 Greene, A., Moriarty, T., Leggatt, W., Ainsworth, T. D., Donahue, M. J., & Raymundo, L.

821 (2023). *Spatial extent of dysbiosis in the branching coral Pocillopora damicornis during an*

822 *acute disease outbreak*. <https://www.researchsquare.com/article/rs-3064933/latest>

823 Haapkylä, J., Unsworth, R. K. F., Flavell, M., Bourne, D. G., Schaffelke, B., & Willis, B. L.

824 (2011). Seasonal rainfall and runoff promote coral disease on an inshore reef. *PLoS One*,

825 6(2), e16893.

826 Heron, S. F., Johnston, L., Liu, G., Geiger, E. F., Maynard, J. A., De La Cour, J. L., Johnson, S.,

827 Okano, R., Benavente, D., Burgess, T. F. R., Iguel, J., Perez, D. I., Skirving, W. J., Strong,

828 A. E., Tirak, K., & Eakin, C. M. (2016). Validation of Reef-Scale Thermal Stress Satellite

829 Products for Coral Bleaching Monitoring. *Remote Sensing*, 8(1), 59.

830 Heron, S. F., Willis, B. L., Skirving, W. J., Eakin, C. M., Page, C. A., & Miller, I. R. (2010).

831 Summer hot snaps and winter conditions: modelling white syndrome outbreaks on Great

832 Barrier Reef corals. *PLoS One*, 5(8), e12210.

833 Howells, E. J., Vaughan, G. O., Work, T. M., Burt, J. A., & Abrego, D. (2020). Annual

834 outbreaks of coral disease coincide with extreme seasonal warming. *Coral Reefs*, 39(3),

835 771–781.

836 Jordan, M. I., & Mitchell, T. M. (2015). Machine learning: Trends, perspectives, and prospects.

837 *Science*, 349(6245), 255–260.

838 Kirk, J. T. O. (1994). *Light and Photosynthesis in Aquatic Ecosystems*. Cambridge University

839 Press.

840 Maynard, J. A., Anthony, K. R. N., Harvell, C. D., Burgman, M. A., Beeden, R., Sweatman, H.,

841 Heron, S. F., Lamb, J. B., & Willis, B. L. (2011). Predicting outbreaks of a climate-driven

842 coral disease in the Great Barrier Reef. *Coral Reefs*, 30(2), 485–495.

843 Meinshausen, N. (2006). *Quantile Regression Forests*.

844 <https://www.jmlr.org/papers/volume7/meinshausen06a/meinshausen06a.pdf>

845 Neely, K. L., Shea, C. P., Macaulay, K. A., Hower, E. K., & Dobler, M. A. (2021). Short- and

846 Long-Term Effectiveness of Coral Disease Treatments. *Frontiers in Marine Science*, 8.

847 <https://doi.org/10.3389/fmars.2021.675349>

848 Oliver, T. H., & Roy, D. B. (2015). The pitfalls of ecological forecasting. *Biological Journal of*

849 *the Linnean Society. Linnean Society of London*, 115(3), 767–778.

850 Palmer, C. V., & Baird, A. H. (2018). Coral tumor-like growth anomalies induce an immune

851 response and reduce fecundity. *Diseases of Aquatic Organisms*, 130(1), 77–81.

852 Pollock, F. J., Lamb, J. B., Field, S. N., Heron, S. F., Schaffelke, B., Shedrawi, G., Bourne, D.

853 G., & Willis, B. L. (2014). Sediment and turbidity associated with offshore dredging

854 increase coral disease prevalence on nearby reefs. *PloS One*, 9(7), e102498.

855 Raymundo L, Andersen M, Moreland-Ochoa C, Castro A, Lock C, Burns N, Taijeron F,

856 Combosch D, Burdick D. (2022). *Conservation and active restoration of Guam's staghorn*

857 *Acropora corals* (168). University of Guam.

858 Raymundo, L. J., Couch, C. S., & Harvell, C. D. (2008). *Coral disease handbook: guidelines for*

859 *assessment, monitoring & management. Coral reef targeted research and capacity building*

860 *for management program*. The University of Queensland St Lucia.

861 Redding, J. E., Myers-Miller, R. L., Baker, D. M., Fogel, M., Raymundo, L. J., & Kim, K.

862 (2013). Link between sewage-derived nitrogen pollution and coral disease severity in Guam.

863 *Marine Pollution Bulletin*, 73(1), 57–63.

864 Renzi, J. J., Shaver, E. C., Burkepile, D. E., & Silliman, B. R. (2022). The role of predators in

865 coral disease dynamics. *Coral Reefs* , 41(2), 405–422.

866 Román, M. O., Wang, Z., Sun, Q., Kalb, V., Miller, S. D., Molthan, A., Schultz, L., Bell, J.,
867 Stokes, E. C., Pandey, B., Seto, K. C., Hall, D., Oda, T., Wolfe, R. E., Lin, G., Golpayegani,
868 N., Devadiga, S., Davidson, C., Sarkar, S., ... Masuoka, E. J. (2018). NASA's Black Marble
869 nighttime lights product suite. *Remote Sensing of Environment*, 210, 113–143.

870 Rosales, S. M., Clark, A. S., Huebner, L. K., Ruzicka, R. R., & Muller, E. M. (2020).
871 Rhodobacterales and Rhizobiales Are Associated With Stony Coral Tissue Loss Disease and
872 Its Suspected Sources of Transmission. *Frontiers in Microbiology*, 11, 681.

873 Ruiz-Moreno, D., Willis, B. L., Page, A. C., Weil, E., Cróquer, A., Vargas-Angel, B., Jordan-
874 Garza, A. G., Jordán-Dahlgren, E., Raymundo, L., & Harvell, C. D. (2012). Global coral
875 disease prevalence associated with sea temperature anomalies and local factors. *Diseases of*
876 *Aquatic Organisms*, 100(3), 249–261.

877 Saha, S., Moorthi, S., Wu, X., Wang, J., Nadiga, S., Tripp, P., Behringer, D., Hou, Y.-T.,
878 Chuang, H.-Y., Iredell, M., Ek, M., Meng, J., Yang, R., Mendez, M. P., van den Dool, H.,
879 Zhang, Q., Wang, W., Chen, M., & Becker, E. (2014). The NCEP Climate Forecast System
880 Version 2. *Journal of Climate*, 27(6), 2185–2208.

881 Selig, E. R., Drew Harvell, C., & Bruno, J. F. (2006). Analyzing the relationship between ocean
882 temperature anomalies and coral disease outbreaks at broad spatial scales. In *Coral Reefs*
883 and *Climate Change: Science and Management*.

884 Shore, A., & Caldwell, J. M. (2019). Modes of coral disease transmission: how do diseases
885 spread between individuals and among populations? *Marine Biology*, 166(4), 45.

886 Skirving, W., Marsh, B., De La Cour, J., Liu, G., Harris, A., Maturi, E., Geiger, E., & Eakin, C.
887 M. (2020). CoralTemp and the Coral Reef Watch Coral Bleaching Heat Stress Product Suite
888 Version 3.1. *Remote Sensing*, 12(23), 3856.

889 Stimson, J. (2011). Ecological characterization of coral growth anomalies on *Porites compressa*
890 in Hawai‘i. *Coral Reefs*, 30(1), 133–142.

891 Sweatman HPA, Cheal AJ, Coleman GJ, Emslie MJ, Johns K, Jonker M, Miller IR and Osborne
892 K. (2008). *Long-term Monitoring of the Great Barrier reef, Status Report* (8). Australian
893 Institute of Marine Science.

894 Vega Thurber, R. L., Burkepile, D. E., Fuchs, C., Shantz, A. A., McMinds, R., & Zaneveld, J. R.
895 (2014). Chronic nutrient enrichment increases prevalence and severity of coral disease and
896 bleaching. *Global Change Biology*, 20(2), 544–554.

897 Walton, C. J., Hayes, N. K., & Gilliam, D. S. (2018). Impacts of a Regional, Multi-Year, Multi-
898 Species Coral Disease Outbreak in Southeast Florida. *Frontiers in Marine Science*, 5.
899 <https://doi.org/10.3389/fmars.2018.00323>

900 Williams, G. J., Aeby, G. S., Cowie, R. O. M., & Davy, S. K. (2010). Predictive modeling of
901 coral disease distribution within a reef system. *PLoS One*, 5(2), e9264.

902 Williams, G. J., Knapp, I. S., Work, T. M., & Conklin, E. J. (2011). Outbreak of *Acropora* white
903 syndrome following a mild bleaching event at Palmyra Atoll, Northern Line Islands, Central
904 Pacific. *Coral Reefs*, 30(3), 621–621.

905 Winston, M., Couch, C., Huntington, B., & Vargas-Ángel, B. (2020). *Ecosystem sciences*
906 *division standard operating procedures: Data collection for rapid ecological assessment*
907 *benthic surveys: 2019 update*. National Marine Fisheries Service, Pacific Islands Fisheries
908 Science Center. <https://doi.org/10.25923/WS5S-KM69>

909 Yoshioka, R. M., Kim, C. J. S., Tracy, A. M., Most, R., & Harvell, C. D. (2016). Linking sewage
910 pollution and water quality to spatial patterns of *Porites lobata* growth anomalies in Puako,
911 Hawaii. *Marine Pollution Bulletin*, 104(1-2), 313–321.

912 **Table 1: Variable inclusion and importance differs for each disease-region model.** The
913 variables tested and selected, as well as their importance, differ for each region (Great Barrier
914 Reef or U.S. Pacific) and disease type (white syndrome or growth anomalies). A cell with a
915 value indicates that the variable was selected for the model and the value represents the percent
916 increase in Mean Squared Error (MSE) of out-of-bag cross-validation predictions across
917 permutations in that predictor variable, with higher values indicating more important predictor
918 variables. (Note that MSE is sensitive to units even though the percent increase in MSE is
919 unitless; thus values for the GBR models that predict disease density will typically be much
920 larger than values for the U.S. Pacific models that predict disease prevalence). x indicates a
921 variable was tested but not selected; a blank cell indicates that the variable was not tested for that
922 model because it is not a hypothesized predictor variable whereas Ø indicates that a variable was
923 not tested because data were not available. Metrics that measure Kd(490) are a proxy for
924 turbidity.

925

926

927

928

929

930

931

932

933

934

Predictor variable	White syndromes		Growth anomalies	
	GBR	U.S. Pac	GBR	U.S. Pac
<i>Time-invariant predictors</i>				
Coral cover	51	0.8	487	x
Median colony size	Ø	2.3	Ø	5.3
Colony size variability			Ø	x
Herbivorous fish density	68	1.2	641	2.3
Parrotfish density	Ø	0.6		
Butterflyfish density	Ø	x		
Long term Kd(490) median	x	2.2	x	1.9
Long term Kd(490) variability	x	1.9	399	x
Coastal development			x	3.1
<i>Seasonally-changing predictors</i>				
Three-week Kd(490) median	x	1.3	350	1.8
Three-week Kd(490) variability	59	1.7	345	x
Month	37	1.1	310	2.5
<i>Regularly-changing predictors</i>				
90-day SST mean			413	5.6
Hot Snap	53	x		
Winter Condition	62	0.8		

935

936

937

938

939 **Fig 1. Methodological overview for model development and weekly update for each disease-**
940 **by-region model.** A) Graphical illustration of Synthetic Minority Over-sampling Technique
941 (SMOTE) where the minority class (i.e., surveys with disease; large gray circles) are used to
942 create synthetic surveys of predictor and response data (i.e., small gray circles) based on k-
943 nearest neighbors (i.e., black lines connecting surveys in n-dimensional parameter space),
944 resulting in approximately equal numbers of surveys with (gray) and without (green) disease
945 present. In this study, we tested different thresholds for inclusion in the minority class. B) We
946 built the model using quantile regression forests, an algorithm that creates many decision trees
947 based on a subsample of predictor variables (example shows each tree using 2 of 3 possible
948 predictor variables), and produces a distribution of target values rather than a mean value. We
949 selected the most parsimonious model across the different SMOTE datasets and quantile
950 regression forests (i.e., with different combinations of predictor variables) based on a withheld
951 portion of the data, using the models with the fewest number of predictor variables with superior
952 predictive skill. The selected models are used in the weekly update for C-E. C) Each week, we
953 update predictor variables for the reef grid. Time-invariant predictor variables are held constant,
954 seasonal predictor variables update each week or month, near-real-time data reflect recent
955 satellite observations, and forecasted data come from 28-member ensemble CFSv2 SST
956 forecasts. D) Using the updated predictor data, we re-run the model to produce a new near real-
957 time prediction and 12 weeks of forecasted data, which we amend to the prior 11 weeks of
958 historical nowcast predictions for a total of six continuous months of disease risk assessments. E)
959 We also vary the predictor data across a gradient of values to produce scenarios, to explore how
960 disease risk changes with different input variable values.

961

962 **Fig. 2 Accuracy of disease nowcast predictions demonstrate improved predictive**
963 **capabilities for V3 compared with its predecessor.** We show comparisons of disease
964 observations (x-axes) with disease predictions (y-axes) for the current model (V3). Points that
965 fall on the gray line indicate a perfect fit between observations and predictions. For white
966 syndromes (left column), we compare disease predictions from V3 with V2 (note that predictions
967 are only available for Hawaii in the U.S. Pacific). For growth anomalies, where no predecessor
968 product exists, we show results for V3 only. V3 predicts disease density (colonies/75m²) for the
969 GBR (top row) and disease prevalence (percent of host colonies exhibiting signs of disease) for
970 the entire U.S. Pacific (bottom row). The V3 product shows the 75th quantile predicted risk
971 (points) and 50th - 90th quantile predictions (lines). V2 predicts risk levels based on Hot Snap
972 values (units = °C-weeks, range = 1-15). The validation data shown in these plots were not used
973 in model creation or training.

974

975 **Fig. 3. Lead time-dependent predictive accuracy and precision of forecasts.** Barplots show
976 predictive accuracy (left column; calculated as difference between 75th quantile prediction and
977 observation) and predictive precision (right column; calculated as difference between 90th and
978 50th quantile predictions) with different lead times (0-12 weeks prior to observation date). In
979 these plots, perfect accuracy and precision marked by horizontal dashed lines indicate zero
980 difference. Results are shown in eight panels for each of the paired disease types (white
981 syndromes and growth anomalies) and regions (GBR, Australia and U.S. Pacific). Predictions (y-
982 axes) calculated as disease density (colonies/75m²) for the GBR and disease prevalence (percent
983 of host colonies exhibiting signs of disease ranging from 0-100%) for the U.S. Pacific. For
984 example, a median value of 10 for the GBR would indicate that, on average, the model predicts

985 10 more colonies as diseased than were observed. Similarly, a median value of -20 in the Pacific
986 would indicate that, on average, the model underpredicts disease prevalence by 20%. The
987 validation data shown in these plots were not used in model creation. Month, seasonal turbidity,
988 and SST metrics varied with lead time (in weeks), while all other predictor variables stayed the
989 same (e.g., benthic characteristics of site).

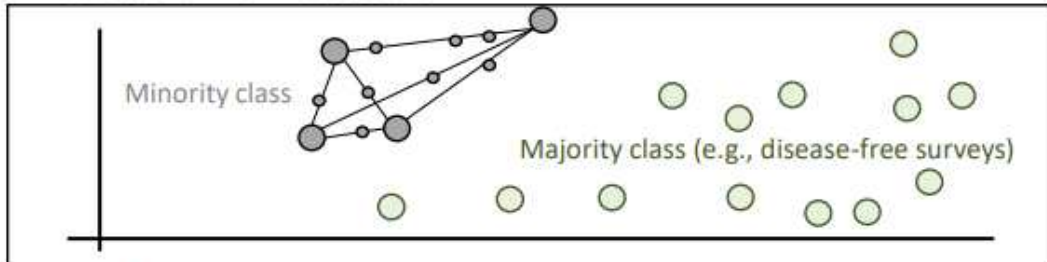
990

991 **Fig 4. Data explorer for Multi-factor Coral Disease Risk product**, accessed on 23 May 2022.

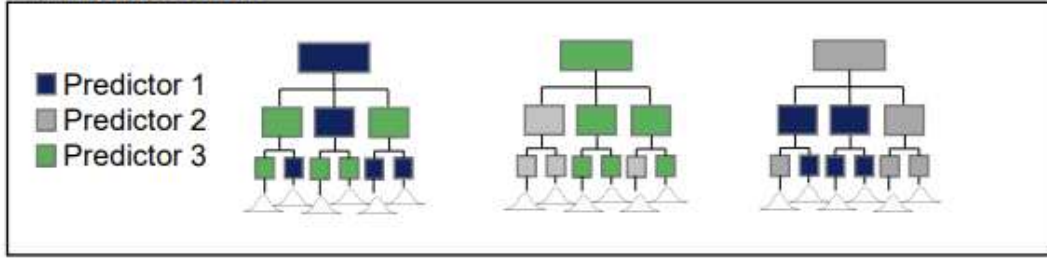
992 A) Spatial view of overall color-coded disease risk nowcast for the Main Hawaiian Islands. The
993 thresholds that separate disease risk levels vary by region and disease type (Appendix S1: Table
994 S1). B) Nowcast risk summary for geographic regions and diseases assessed. C) Pixel-specific
995 time-series of nowcasted and forecasted risk on the south coast of Lanai (white arrow in panel A)
996 for growth anomalies and white syndromes, over a 5-month time period.

997

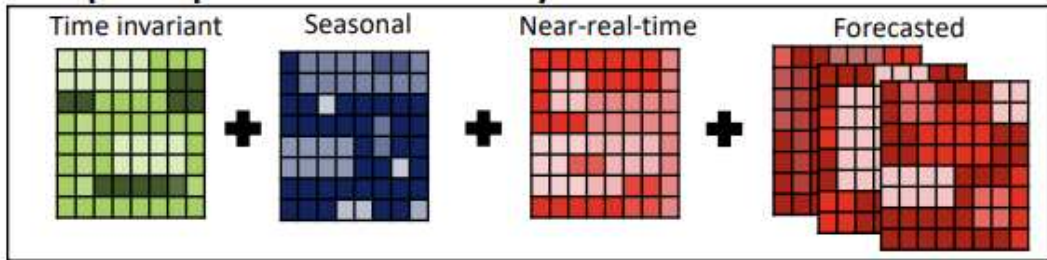
A. Create SMOTE dataset



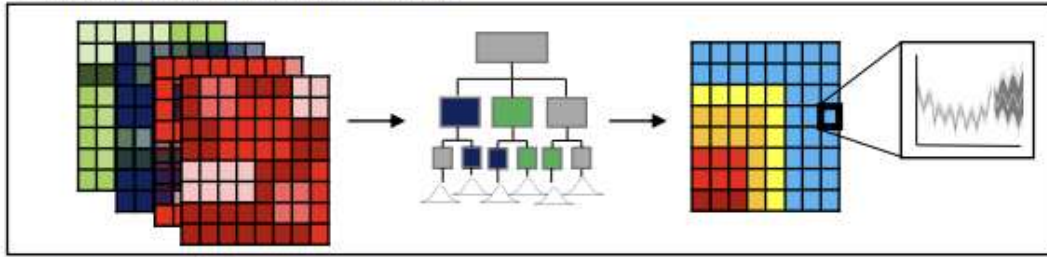
B. Build model



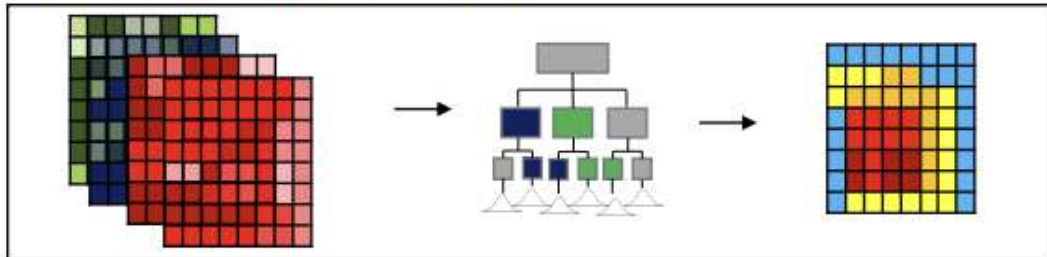
C. Update predictor data weekly



D. Run model on new data

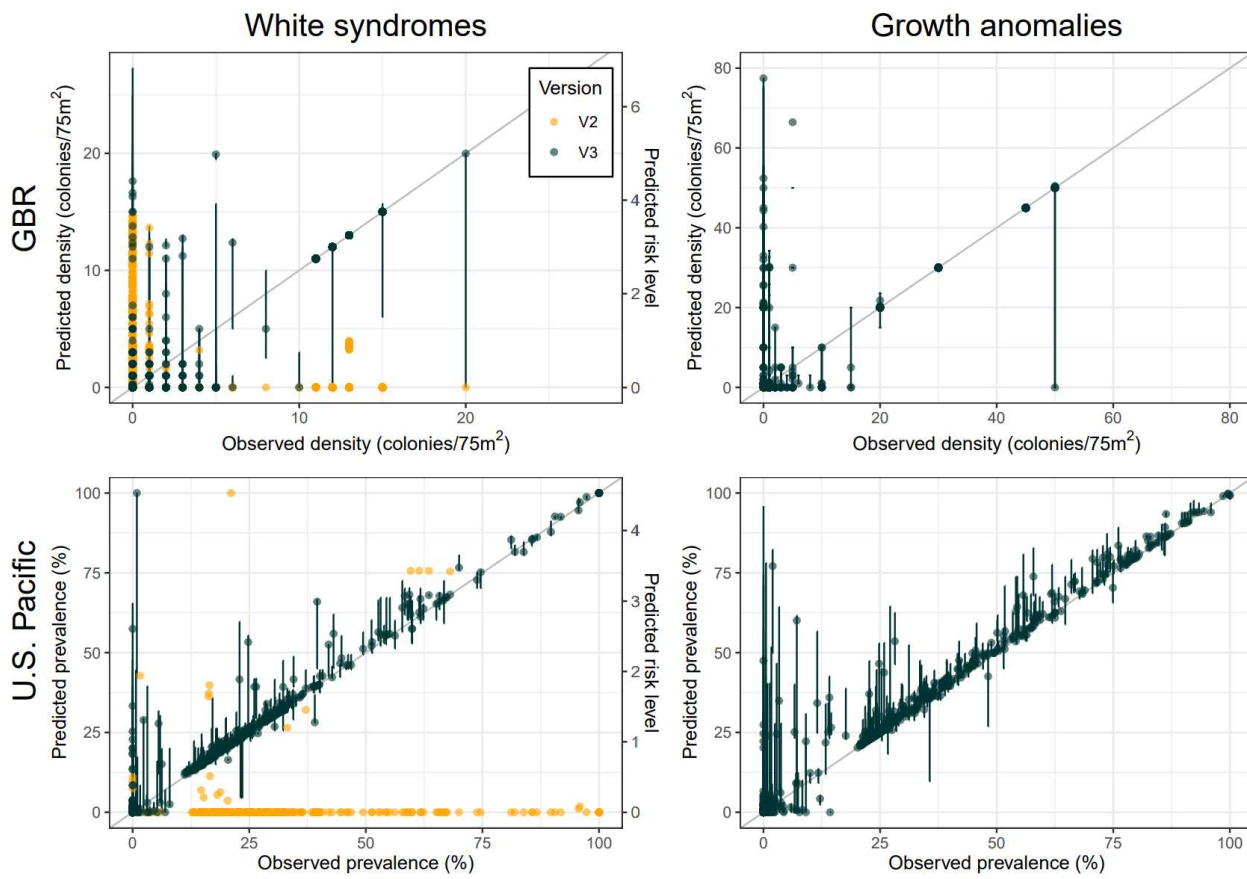


E. Run model on new scenarios



998

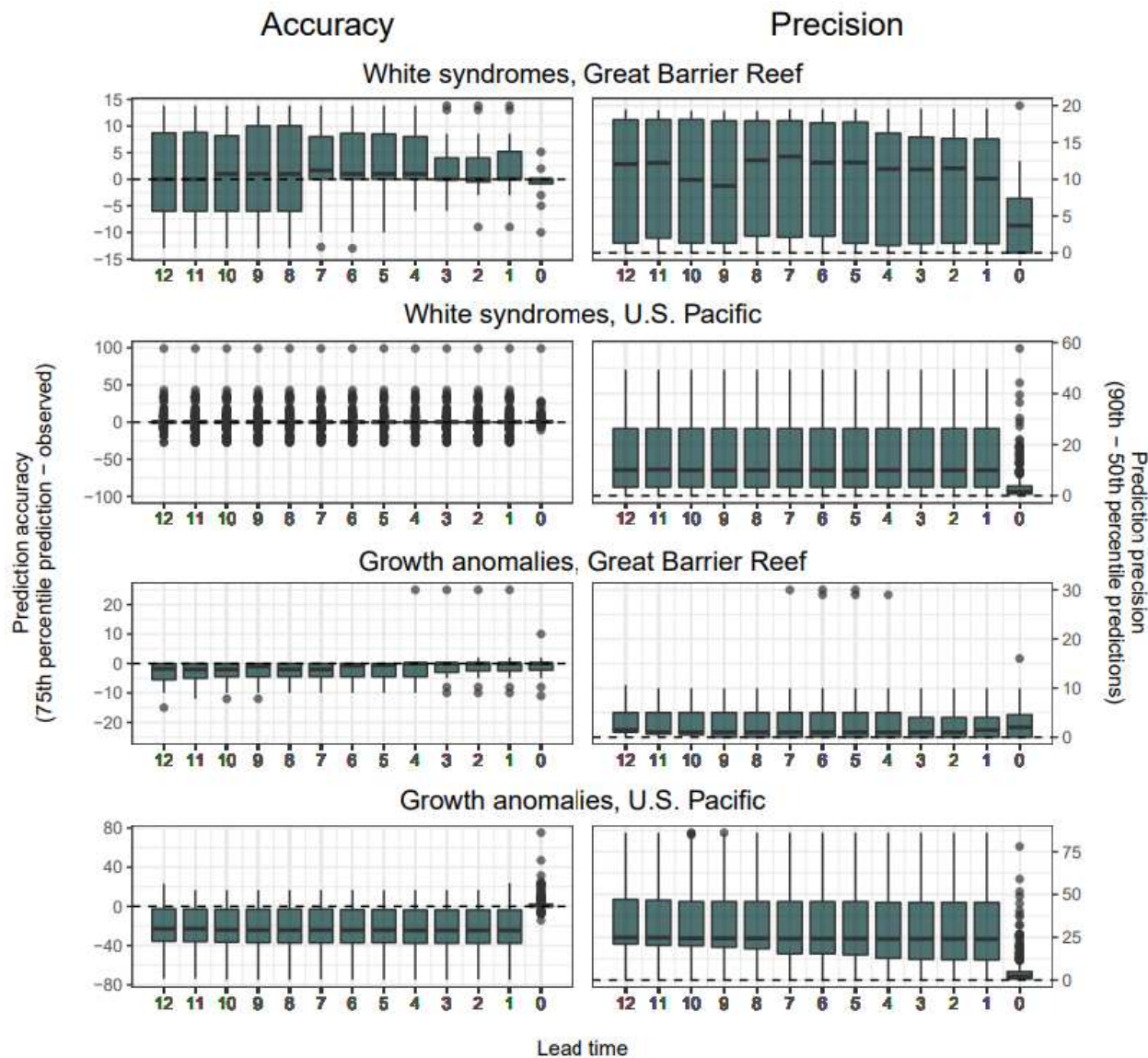
999 **Figure 1**

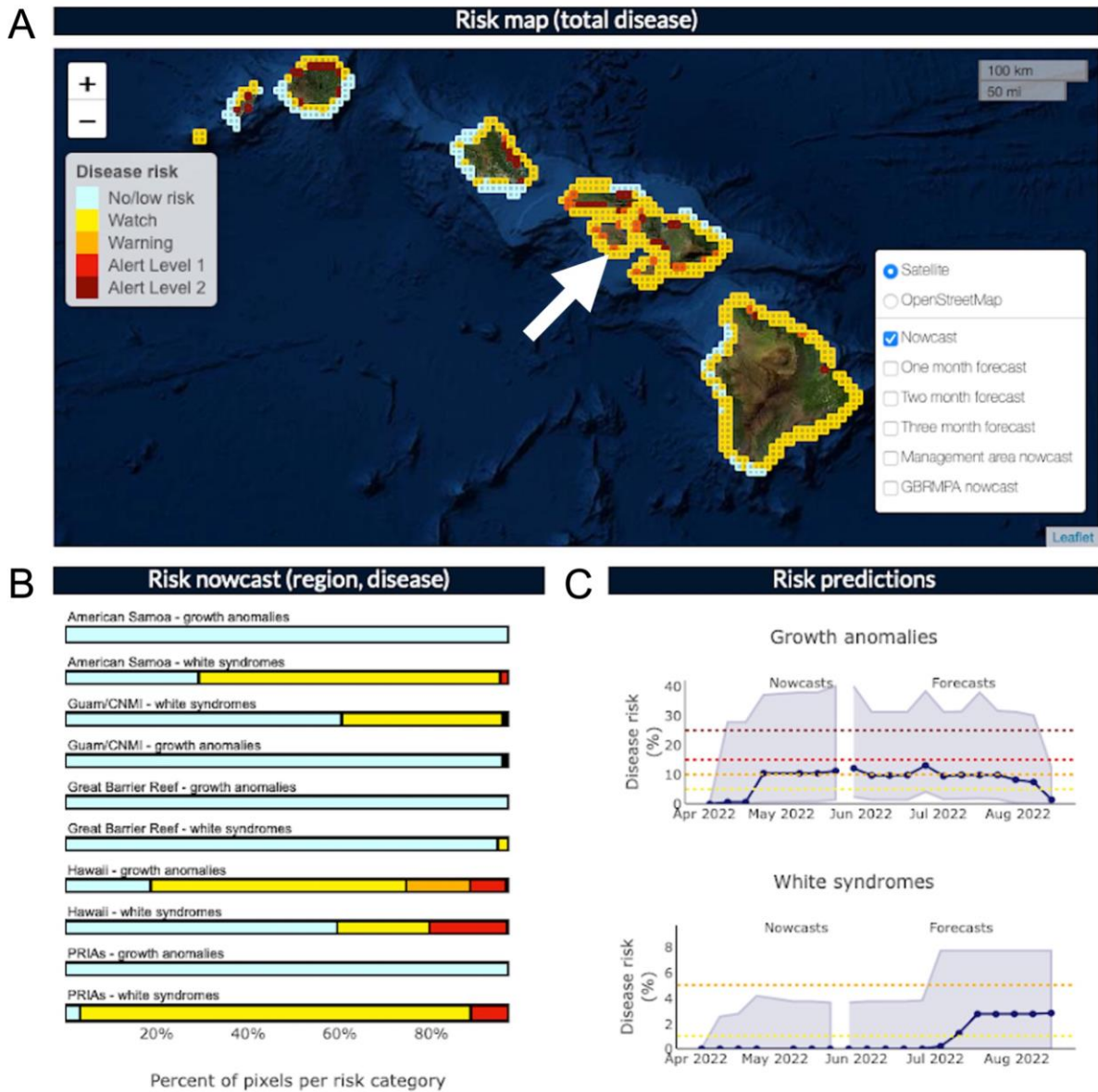


1000

1001 **Figure 2**

1002





1006

1007 **Figure 4**